Gene Expression, Mutation, and Structure−Function Relationship of Scorpion Toxin BmP05 Active on SK_{Ca} Channels†

Jing-Jiang Wu,‡ Lin-Lin He,§ Zhuan Zhou,§ and Cheng-Wu Chi*,‡

State Key Laboratory of Molecular Biology, Shanghai Institute of Biochemistry and Cell Biology, and Institute of Neuroscience, Chinese Academy of Sciences, Shanghai 200031, China

Received June 29, 2001; Revised Manuscript Received December 3, 2001

ABSTRACT: Four peptide inhibitors of small-conductance Ca^{2+}-activated, apamin-sensitive K^+ channels (SK_{Ca}) have been isolated from the venom of the Chinese scorpion *Buthus martensi*, named BmP01, BmP02, BmP03, and BmP05, respectively [Romi-Lebrun, R. (1997) *Eur. J. Biochem. 245*, 457−464]. Among them BmP05 with 31 amino acid residues has been intensively studied due to its most potent toxicity. To investigate the structure−function relationship of BmP05, its wild type and seven mutants (their C-termini unamidated) were successfully expressed in the yeast secretion system and purified with a high yield over 8 mg/L. Their toxicity to mice and electrophysiological activity on the K^+ currents (SK_{Ca} and Kv) in rat adrenal chromaffin cells were measured and compared. The results indicated the following: (1) As a selective antagonist against SK_{Ca}, 1 μM rBmP05 is equivalent to 0.2 μM apamin, and its IC_{50} is 0.92 μM. (2) The basic residues Lys and Arg located at positions 6 and 13 in the N-terminal α-helix region are essential and synergetic in the interaction of the toxin with SK_{Ca}. (3) Disruption of the α-helix by mutation of Gln at position 9 with Pro results in almost total loss of toxicity. (4) The C-terminal residue His31 plays an auxiliary role in the interaction of the toxin with SK_{Ca}. (5) The β-turn connecting two β-sheets near the C-terminal part is responsible for the specificity of the toxin to the different subtypes of K^+ channels.

Potassium channels form a large family of integral membrane proteins that are present in almost every living cell. They play a key physiological role by setting the resting potential and shaping bioelectric signals in excitable and nonexcitable cells. The study of K^+ channels is of high value for the understanding of many physiological processes. Rat adrenal chromaffin cells (RACC)[1] express SK_{Ca} channels (*2*), which produce slow after-hyper-polarization and play an important role in spacing action potentials and in limiting the frequency of repetitive firing.

More than a hundred neurotoxins have been isolated and identified from the venom of scorpions belonging to the *Buthidae* family. Most of the long-chain scorpion peptides composed of 60−70 amino acid residues are modifiers of voltage-gated Na^+ channels, while most of the short-chain scorpion peptides composed of 30−40 residues have been characterized to be blockers of K^+ channels (*3*, *4*). These toxins can be roughly classified into several groups according to their primary sequences and their not very strict specificities to the subtypes of K^+ channels (*5*). Among them, toxins specifically active on low-conductance, Ca^{2+}-activated K^+ channels and sharing less structure homology with others have been widely studied, such as LeTx1 from *Leiurus quinquestriatus hebraeus* (*6*), P05 from *Androctomus mauretanicus mauretanicus* (*7*), and BmP05 from *Buthus martensi* Karch (*1*).

The toxins LeTx1 and P05 have been studied thoroughly on their primary sequences (*6*, *7*), structure conformations (*8*, *9*), chemical syntheses (*10*, *11*), and structure−function relationships (*11*−*13*). They are peptides of 31 residues with three disulfide bridges, composed of an α-helix from residue 5 to residue 14 and two antiparallel β-sheets (residues 17−22 and 25−29) joined by a β-turn from residue 22 to residue 25 (Figure 1) (*8*, *9*).

Unlike the other groups of toxins against Kv or BK_{Ca} channels, whose functional sites are located in the β-sheets near the C-termini of the toxins (*5*), a positively charged area in the N-terminal α-helix is important for the activity of the SK_{Ca} toxins LeTx1 and P05 (*11*−*13*). These toxins are capable of competing with apamin for SK_{Ca} channels due to their similar basic residue sequence though this sequence in apamin is in the opposite position at the C-terminal part (*1*).

BmP05, a scant component of *B. martensi* Karch venom (only 0.01% of dry venom mass), is structurally and functionally similar to LeTx1 and P05 (*1*). Its genomic structure was elucidated recently (*14*). In the present paper, we describe the site-selected point mutation of BmP05, the gene expression in the yeast secretion system, and the study on structure−function relationship based on the toxicity to

† This work was supported by funds from 973 program G1998051121, G2000077800, and NSFC (39525009).

* To whom correspondence should be addressed. Tel: 86-21-64337152. Fax: 86-21-64338357. E-mail: Chi@sunm.shcnc.ac.cn.

‡ State Key Laboratory of Molecular Biology, Shanghai Institute of Biochemistry and Cell Biology.

§ Institute of Neuroscience.

[1] Abbreviations: SK_{Ca} channels, small-conductance, Ca^{2+}-activated K^+ channels; CD, circular dichroism; RACC, rat adrenal chromaffin cell; MW, molecular weight; MFα, mating factor α; TEA, tetraethylammonium chloride.

10.1021/bi011367z CCC: $22.00
Published on Web 01/30/2002

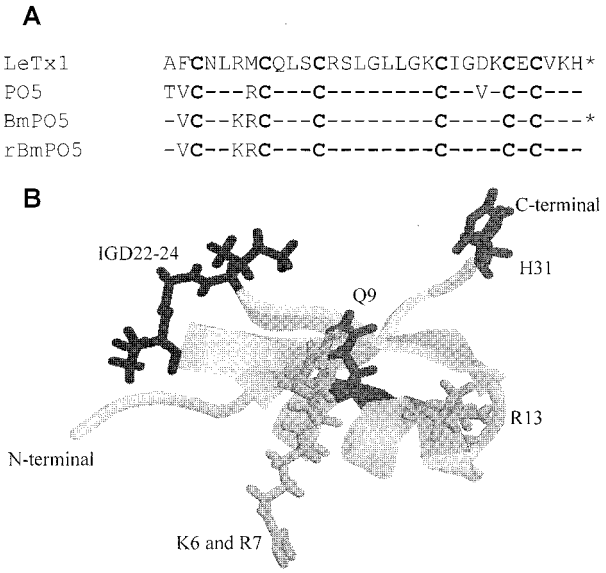

FIGURE 1: Structures of scorpion SK_{Ca} toxins. (A) Primary structures of BmP05 and its analogues: LeTx1 from *L. quinquestriatus hebraeus* (*23*), P05 from *A. mauretanicus mauretanicus* (*7*), and BmP05 from *B. martensi* Karsch (*1*). (B) Three-dimensional structure of P05-NH_2 (*9*), viewed by rasmol software; the corresponding residues to be mutated in rBmP05 are indicated in stick format.

mice and the electrophysiological effect on RACCs using whole-cell patch-clamp recording.

MATERIALS AND METHODS

Materials

Escherichia coli strain DH5α was used for production of plasmids. *Saccharomyces cerevisiae* strain S78 (Leu2, Ura3, Rep4) and vector pVT102U/α (gifts from Dr. You-shang Zhang, Shanghai Institute of Biochemistry, China) were used for expression of BmP05; uracil-deficient YSD and YPD media (*15*) were used for propagation of yeast transformants. Enzymes used for DNA manipulation were purchased from Promega (U.S.A.), the chromatography media from Pharmacia Biotech (Sweden), and HPLC C-18 columns (4.6 × 250 mm) from Waters (U.S.A.). PCR primers were synthesized in an Applied Biosystems DNA synthesizer 380-A (Perkin-Elmer), and other chemicals were of analytical reagent grade. The mice used for toxicity bioassay were male Kunming mice with a body weight of 20 ± 2 g.

Methods

Construction of Expression Plasmids. The expression plasmid pVT102U/α-BmP05 was constructed on the basis of the cDNA sequence of BmP05 (*14*) (Figure 2). P1 was used as a sense primer with an *Xba*I restriction site (5′-CG TCTAGAT AAA AGA GCA GTT TGT AAT C-3′), corresponding to two additional basic residues Lys-Arg, a site for the enzymatic cleavage by the yeast kexin, and the first four residues (Ala-Val-Cys-Asn) of the mature peptide. P2 was used as an antisense primer (5′-CG AAGCTTA GTG TTT AAC ACA TTC GCA-3′) with a *Hin*dIII restriction site, corresponding to the last six residues (Cys-Glu-Cys-Val-Lys-His) of the mature peptide. Using M13mp18-BmP05 (*14*) as a template, the amplified product was precipitated, digested with *Xba*I and *Hin*dIII, and then cloned into the expression plasmid pVT102U/α.

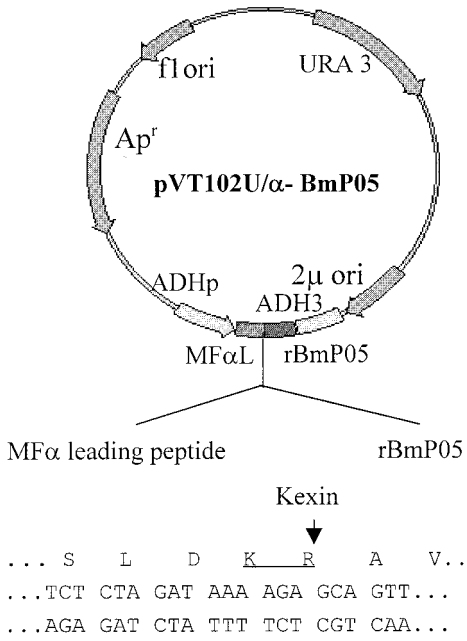

FIGURE 2: Construction of the expression plasmids. The genes encoding the mature peptide of BmP05 or its mutants were cloned into the expression vector pVT102U/α. The gene was downstream of the gene encoding the leading peptide of yeast mating factor α. The additional residues Lys-Arg between the leading peptide and the toxin was designed for the enzymatic cleavage by the yeast kexin.

The expression plasmids of BmP05 mutants were also constructed as follows: The gene encoding mutant H31A was amplified by one-step PCR using pVT102U/α-BmP05 as a template. P1 was paired with the antisense primer P3 (5′-CGAAGCTTA **GGC** TTT AAC ACA-3′) containing a *Hin*dIII restriction site, a stop codon, and codons for the last four residues (Cys-Val-Lys-**Ala**). The amplified product was precipitated, digested with *Xba*I and *Hin*dIII, and then cloned into the expression plasmid pVT102U/α. The genes encoding mutants K6A, Q9P, IGD22−24MNG, and K6A/R13A were obtained by two steps of PCR. In the first step PCR of K6A, P2 was paired with the sense primer P4 (5′-GCA GTT TGT AAT CTT **GCC** AGA-3′) corresponding to the first seven residues of K6A using pVT102U/α-BmP05 as a template. To avoid interference from the original template, the amplified product was precipitated and cloned into vector pGEM-T. Then pGEM-T-K6A was used as a template for the second PCR with a pair of primers, P1 and P2; the product of the second PCR was precipitated and digested with *Xba*I and *Hin*dIII and cloned into the expression plasmid pVT102U/α. Since the same strategy was used for other mutants in the second PCR, only the template and primers in the first PCR are given as follows. For Q9P, the template was pVT102U/α-BmP05, and the pair of primers were P2 and the sense primer P5 (5′-TGT AAT CTT AAA AGA TGT **CCG**-3′) corresponding to residues 3−9 of Q9P (Cys-Asn-Leu-Lys-Arg-Cys-**Pro**). For IGD22−24MNG, the template was pVT102U/α-BmP05, and the pair of primers were P1 and the antisense primer P6 (5′-AAC ACA TTC GCA TTT **CCC ATT CAT**-3′) corresponding to residues 22−29 of IGD22−24MNG (**Met-Asn-Gly**-Lys-Cys-Glu-Cys-Val). For K6A/R13A, the template was pVT102U/α-R13A, and the

primers were P2 and P4. The mutant R13A was obtained using three steps of PCR. In the first PCR, the template was pVT102U/α-BmP05, the primers were P2 and the sense primer P7 (5′-AGA TGT CAG TTA TCT TGT **GCA** TCA-3′) corresponding to residues 7−14 of mutant R13A (Arg-Cys-Gln-Leu-Ser-Cys-**Ala**-Ser), and the amplified product was purified and cloned into pGEM-T vector. For the second PCR, the above plasmid was used as a template with P2 and the sense primer P8 (5′-GTT TGT AAT CTT AAA AGA TGT CAG TT-3′) corresponding to residues 2−10. The amplified product was directly used as template for the third PCR, in which the primers were P1 and P2; the amplified product of the third PCR was precipitated, digested with *Xba*I and *Hin*dIII, and then cloned into the expression plasmid pVT102U/α.

Gene Expression of Constructed Plasmids. The constructed plasmid confirmed by DNA sequencing was transformed into *S. cerevisiae* S78 in terms of the LiCl method. One positive transformant on the YSD plate was cultured in 50 mL of YSD liquid media overnight and then transferred to 1 L of YPD media for 3 day cultivation.

Purification of Recombinant BmP05 and Its Mutants. One liter of YPD culture was centrifuged at 4000*g* for 20 min. The pH of the supernatant was adjusted to pH 7.5 with 2 N NaOH. The solution was then applied onto a DE-22 column (2 × 20 cm) previously equilibrated with 30 mM Tris·HCl buffer (pH 7.5) at a flow rate of 1.2 mL/min. The breakthrough was collected, and its pH was adjusted to 4.5 with 1 N HOAc. Then the solution was applied on a CM-32 column (2 × 20 cm) previously equilibrated with 35 mM NaOAc/HOAc buffer (pH 4.5) at a flow rate of 1.0 mL/min. After being washed with the same buffer, the chromatography was developed by a stepwise elution with increasing concentrations of NaCl (0.1, 0.25, and 0.5 M) in the equilibration buffer. For the recombinant BmP05 and its mutants Q9P and IGD22−24MNG, they were not eluted out until 0.5 M NaCl was used. For the mutants K6A, R13A, K6A/R13A, and H31A, they emerged in the 0.25 N NaCl elution due to the reduction in positive charge caused by the Ala replacement. The collected fraction of interest was further purified on the HPLC C-18 column equilibrated with 0.1% TFA and eluted with a linear gradient of acetonitrile in 0.1% TFA. The peak of the recombinant toxin was then pooled, lyophilized, and rechromatographed on the HPLC C-18 column.

Tricine−SDS−PAGE Electrophoresis. The experiments were performed as described (*16*).

Mass Spectra. The molecular weights of rBmP05 and its mutants were measured by LC-MS on HP1100 filtration system and Finnigan LCQ ion trap.

Circular Dichroism (CD) Spectroscopy. The protein samples with concentration of 0.2 mg/mL were measured on a Jasco J-715 spectropolarimeter with nitrogen purge at room temperature. A 0.1 cm path-length cuvette was used, and spectra were accumulated over three scans.

Toxicity Bioassay and LD_{50} Determination. Toxic activity was tested on Kunming mice. The lyophilized recombinant toxin was dissolved in a solution of 0.9% NaCl and 1 mg/mL BSA. Mice were divided into five groups and given different doses (nanograms of toxin/gram of mouse); each group consisted of 5−10 mice with the same dose. Five microliters of the toxin solution was administrated via intracerebroventricular injection. For the control only the buffer solution was injected. After 2 h the percentage of dead mice in each group was calculated and transformed into the reaction rate. A plot of reaction rate versus log dose was made. The dose corresponding to the reaction rate 5.0 from the regression straight line was the LD_{50} value of the measured toxin.

Cell Cultures. Rat adrenal medulla chromaffin cells were prepared as described previously (*17*). Briefly, adult Wister rats of 250−300 g were used. All individual cells were obtained after 40 min digestion in the enzyme solution. The cells were cultured with DMEM in a CO_2 incubator. The cells cultured for 1−4 days were used in experiments.

Electrophysiological Experiments. The standard external solution in the bath contains (mM) 125 NaCl, 2.8 KCl, 10 $CaCl_2$, 1 $MgCl_2$, and 10 HEPES, pH 7.4. The 0 Ca bath solution is the same as the standard solution, except 10 mM Ca^{2+} is replaced by NaCl. The standard internal solution in the patch pipet contains (mM) 145 KCl, 8 NaCl, 1 $MgCl_2$, and 10 HEPES and nystatin, 250 μg/mL, pH 7.2. The toxin was dissolved in the standard external solution.

The voltage-gated membrane currents were recorded under whole-cell voltage clamp using the nystatin perforated patch-clamp technique (*18*). Experiments were performed by using Axon 200B (Axon Instruments, Foster City, CA) or the PC-2B (INBIO Inc., Wuhan, China) patch-clamp amplifier with a pClamp 8 data acquisition system. Data were analyzed with Igor software (AveMatrix, Lack Oswego, OR). The toxin sample was puffed to the cell through the perfusion system. All experiments were carried out at room temperature (22−25 °C). The control/wash solution and the solution with the toxin of interest were puffed locally to the cell under recording via RCP-2B multichannel micro perfusion system (INBIO Inc., Wuhan, China), which has a fast exchange time (<100 ms) for electronic switching between seven solution channels. The puffing pipet of 100 μm tip diameter is located about 120 μm from the cell. The patch-clamp data are given as mean ± SD. For the significant test we used the *t*-test. For fit of the dose curve, we used the standard Hill equation $Y = Y_m/[1 + (K_d/C)^n]$. Here Y is effect, Y_m is maximum effect of the drug, K_d is dissociation constant, C is concentration of the drug, and n is Hill coefficient. The IGOR Pro software (WaveMatrix, OR) is used for data analysis and graphs.

RESULTS AND DISCUSSION

Construction of the Expression Plasmids and Gene Expression of BmP05 and Its Mutants. Using PCR, the gene coding for the mature peptide of BmP05 was amplified with two additional residues Lys-Arg upstream of its N-terminus; this pair of basic residues is necessary for the yeast kexin to cleave the fusion protein. After being digested with *Xba*I and *Hin*dIII, the amplified gene was then inserted into the expression plasmid pVT102U/α just downstream of the gene coding for the leading peptide of the yeast mating factor α (MFα). The plasmid was then transformed into yeast S78. After being cultured for 3 days in YPD media, a good harvest of the recombinant rBmP05 could be found in the supernatant. The construction of expression plasmids for other mutants was the same as for rBmP05. It is worth pointing out that there is no enzyme catalysis system for the C-terminal amidation of protein in the yeast expression; thus,

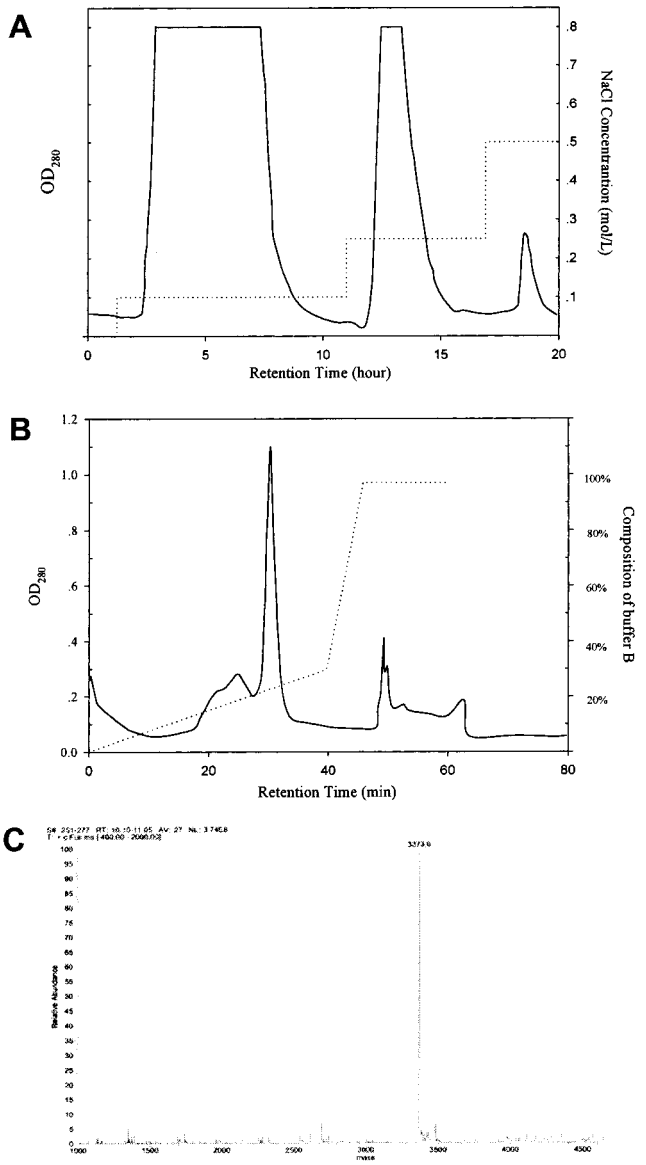

FIGURE 3: Purification of rBmP05. (A) The breakthrough from DE-22 was chromatographed on CM-32 (column 2 × 20 cm), and the rBmP05 fraction was eluted with a buffer of 0.5 N NaCl, pH 4.5, at a flow rate of 1.0 mL/min. (B) The collected fraction eluted from CM-32 was further purified on HPLC and eluted at the retention time of 30 min. Conditions: buffer A, 0.1% TFA; buffer B, 70% acetonitrile and 0.1% TFA; flow rate, 1.0 mL/min with a slow gradient elution increasing at 0.5% acetonitrile per minute. (C) Mass spectra of rBmP05. The calculated MW of rBmP05 was 3373.1; the measured MW was 3373.0.

different from the native BmP05, its recombinant wild-type rBmP05 and all its mutants were not amidated at their C-terminus.

It is interesting to point out that some SK_{Ca} scorpion toxins such as LeTx1 (*10*) and BmP05 (*1*) are amidated at their C-termini, while P05 is not (*11*).

Purification of the Recombinant BmP05 and Its Mutants. The expressed rBmP05 or its mutants in 1 L of YPD culture were first applied on DE-22 at pH 7.5 to remove bulk contaminant and negatively charged dark pigments in YPD media. The breakthrough of DE-22 was then subjected to cation chromatography on CM-32, and the fraction of interest was further purified on HPLC (Figure 3). About 8−10 mg of rBmP05 from 1 L of culture was obtained. For the mutant

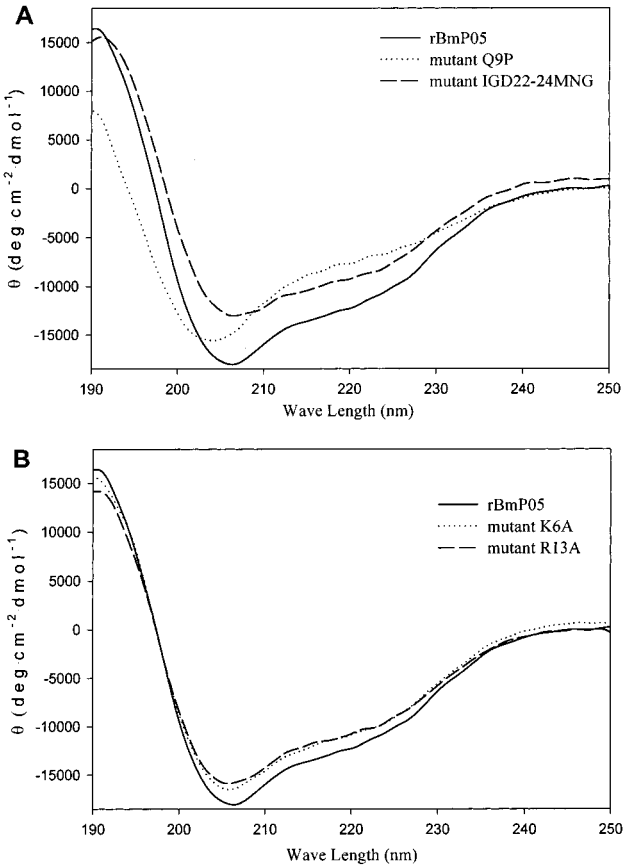

FIGURE 4: CD spectra of rBmP05 and its mutants. (A) CD spectra of rBmP05 and its mutants Q9P and IGD22−24MNG. (B) CD spectra of rBmP05 and the mutants K6A and R13A.

K6A/R13A, the yield even reached 20 mg/L, which was much higher than 0.15−3.5 mg/L of other recombinant scorpion K^+ channel toxins ever reported in the literature (*19*−*21*). Thus, the yeast expression system has prominent advantage of the high yield, easy purification, and needlessness of disulfide refolding.

Molecular Weight Determination of rBmP05 and Its Mutants by Mass Spectra. The measured molecular weights (MW) of rBmP05 and its mutants agreed well with the calculated ones (data not shown), indicating that the recombinant products were no other than the real ones which were expected to be expressed.

CD Spectra of rBmP05 and Its Mutants. The CD spectra of rBmP05 and its mutants K6A, Q9P, R13A, IGD22−24MNG are presented in Figure 4. The curves of the mutants K6A and R13A showed no apparent difference from that of rBmP05, while obvious changes in spectra were found in the mutants Q9P and IGD22−24MNG. This implied that the α-helix and loop conformations might be distorted by substitution with Pro at position 9 and with MNG at positions 22−24, respectively.

Toxic Activity. The determined LD_{50} of the expressed rBmP05 and its mutants are shown in Table 1. The LD_{50} value of rBmP05 was 66 ng/mouse (3.3 ng/g of mouse), higher than 37 ng/mouse for the native BmP05 as described previously (*1*). This might be explained by the fact that the C-terminal amidation of the toxin may also have some significance for the toxicity or the amidated toxin is more resistant for exopeptidase degradation. It is also worth pointing out that the binding affinity of the C-terminal

Table 1: Toxicity of BmP05 and Its Mutants

mutant	LD_{50} (ng/g of mouse)	relative toxicity (%)
rBmP05	3.3	100
K6A	24.3	13.6
Q9P	131.8	2.5
R13A	19.3	17.0
IGD22−24MNG	10.45	31.6
H31A	7.39	44.6
K6A/R13A	undetectable	undetectable

amidated P05 for the apamin receptor was much higher than that of the C-terminal free P05 (*9*). The toxicity of the mutants K6A and R13A decreased to 13.6% and 17%, respectively. These basic residues R6 and R13 in LeTx and P05 were also reported to be important for their toxicities and competitive activities with apamin (*11*−*13*). If both residues were substituted with Ala, the toxicity of the mutant was totally undetectable. The results were also confirmed by electrophysiological experiments (data not shown), indicating that these two basic residues in the α-helix are not only essential but also synergetic for the toxicity.

Replacement of the residue Gln at position 9 with Pro (a very strong α-helix breaker) resulted in a great change in the conformation of the toxin, which was verified by the CD spectra. As expected, the toxicity of the mutant dramatically dropped to 2.5%. Thus, we provided direct evidence to elucidate the relationship between the α-helix structure and activity of the toxin though it has been predicted that the α-helix of the toxin is believed to interact with its receptor (*9*, *11*). The mutation at the C-terminal residue His with Ala led to loss of half the toxicity (Table 1). It implied that the C-terminal His has an auxiliary effect if not essential on the activity of the toxin.

Electrophysiology Assay. In addition to many voltage-gated Na^+, K^+, and Ca^{2+} channels, RACC has prominent small-conductance Ca^{2+}-activated potassium channels (SK_{Ca} channels) (*2*). Thus, to verify whether rBmP05 has an effect on the SK_{Ca} channel, the cultured rat adrenal chromaffin cells were used. Figure 5A provides the patch-clamp protocol recording pure SK_{Ca} currents in RACCs. The slow tail SK_{Ca} currents were activated at −100 mV after a 1 s depolarization prepulse conditioning step to 0 mV for the Ca^{2+} influx through the Ca^{2+} channel (*2*, *22*). Figure 5B shows the effect of rBmP05 and apamin on SK_{Ca} currents using the same protocol as in Figure 5A. Their block effects could be washed out nearly completely. It has been reported that the bee toxin apamin specifically blocks SK_{Ca} currents in chromaffin cells (*2*). This experiment indicated that 1 μM rBmP05 gave an effect similar to that of 0.2 μM apamin on the block of SK_{Ca} in RACC (48.5 ± 3.1%, $n = 27$). The dose curve in Figure 5C showed that the IC_{50} value is 0.92 μM for rBmP05 and the Hill coefficient against SK_{Ca} is 0.95. This implied that a single binding site between the RACC SK_{Ca} channel and rBmP05 was responsible for the block.

In other scorpion voltage-gated K^+ channel toxins, there is a conserved sequence MNGK in the β-turn between two antiparallel β-sheets. We wonder whether this sequence is related with the specificity of the toxins for their corresponding subtypes of the K^+ channel and whether the mutant IGD22−24MNG could also block Kv besides SK_{Ca} currents. Figure 6A shows the effect of this mutant on SK_{Ca} currents.

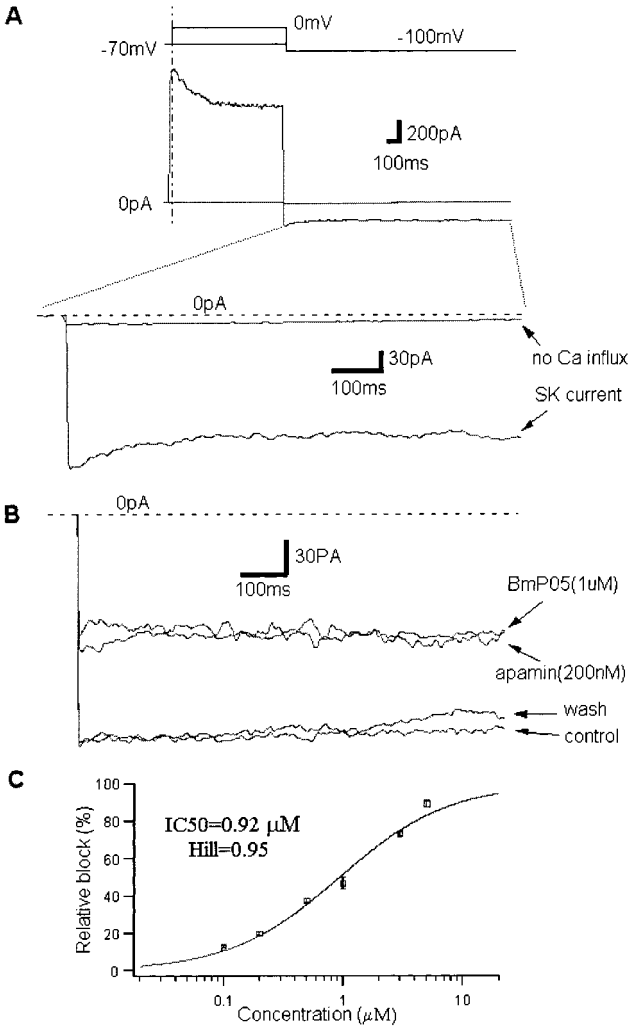

FIGURE 5: Effects of rBmP05 and apamin on SK_{Ca} channels in rat adrenal chromaffin cells (RACCs). (A) A protocol to record SK_{Ca} currents in a rat adrenal chromaffin cell. The slow tail current was elicited at −100 mV either with or without a 1 s conditioning step to 0 mV ($n = 4$). (B) Block effects of BmP05 and apamin on SK_{Ca} channels. The experimental protocol of panel A is applied while puffing control, rBmP05, control, and apamin one after another with 180 s intervals between two successive recordings (the access resistance R_s is reduced to less than 20 mΩ). 1 μM rBmP05 or 200 nM apamin gave almost 50% block of SK_{Ca} currents ($n = 27$). (C) Dose effects of rBmP05. The curve was fitted well with Hill = 0.92 and K_d (or IC_{50}) = 0.92 μM. 5−27 cells were used for different concentrations.

The block effect could also be washed out nearly completely. However, compared with the wild-type rBmP05, the block effect was relatively low. A 15 μM quantity of the mutant was needed to block 72.1 ± 3.3% of SK_{Ca} in RACC ($n = 13$). According to the dose curves of rBmP05 (Figure 5C) and the MNG mutant (Figure 6D), the mutant ($IC_{50} = 2.2$ μM) was 2.5 times less potent for SK_{Ca} than its wild type ($IC_{50} = 0.92$ μM). Being approximated to the toxicity assay, the toxicity of the mutant was around three times lower (Table 1).

Figure 6B shows the effect of the mutant IGD22−24MNG on Kv currents in 0 mM Ca^{2+} bath solution, under the conditions that all Ca^{2+}-dependent currents including SK_{Ca} and BK_{Ca} were absent (*2*). The Kv currents were elicited by depolarization to +20 mV from a holding potential of −70 mV. The experiments showed that the maximum block of

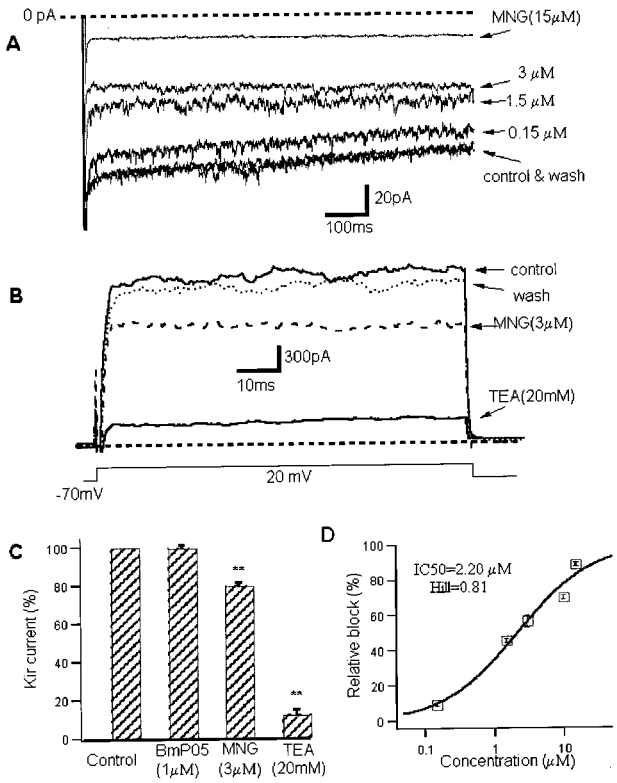

FIGURE 6: Effects of the mutant IGD22−24MNG on SK_{Ca} and Kv currents in RACCs. (A) Effect of the mutant on SK_{Ca} currents recorded with the same protocol as in Figure 5. (A) 15 μM mutant blocked 72 ± 3% of SK_{Ca} currents (n = 13). (B) Effect of the mutant on Kv currents. The Ca-activated K^+ currents were blocked by the 0 mM Ca^{2+} bath solution. The Kv currents were elicited by a step to 20 mV from the holding potential. 3 μM mutant blocked 20 ± 2% of Kv current (p < 0.01, n = 15). In the same cell 20 mM TEA blocked 88 ± 4% of Kv current (p < 0.01, n = 3). (C) Effect of rBmP05 and the mutant on Kv currents. Experiment conditions were same as in (B). rBmP05 showed no effect on Kv currents in the same cells. (D) Dose effects of the MNG mutant. The curve was fitted with Hill = 0.81, K_d (or IC_{50}) = 2.20 μM. 4−7 cells were used for different concentrations.

Kv channels in RACC was 20 ± 2% with 3 μM mutant (n = 15, p < 0.01). The block could not be increased more even using 15 μM mutant (data not shown). As shown in Figure 6B,C, TEA, a classical Kv blocker (*24*), could block 88 ± 4% of the depolarization-induced outward current in the same cells (n = 3, p < 0.01). This confirmed that the MNG-sensitive component was indeed a Kv current. On the contrary, rBmP05 gave no effect on Kv currents (Figure 6C) (n = 5, p < 0.01). The dose curve of the MNG mutant (Figure 6D) showed that the IC_{50} was 2.20 μM for MNG mutant and the Hill coefficient against SK_{Ca} is 0.81. This implied that probably the same single binding site of RACC SK_{Ca} for rBmP05 was also for the MNG mutant. Thus, this mutation caused two effects: reducing the affinity of the SK_{Ca} binding site and creating a new binding site between the NMG mutant and the voltage-sensitive Kv channel.

The present structure−function study of the scorpion toxin BmP05 is based on both the toxicity tests and electrophysiological experiments. Their results paralleled well with each other (not all data shown). The technique of protein engineering used in this paper made it possible to elucidate the contribution of a definite residue to the function of toxin. The results gave a general view of the structure−function relationship of the scorpion SK_{Ca} toxins. On the basis of this knowledge, a toxin with a new function might be designed and created using such a peptide scaffold. Furthermore, this paper provides a clue to a better understanding of the molecular basis of the important SK_{Ca} channels.

REFERENCES

1. Romi-Lebrun, R., Martin-Eauclaire, M. F., Escoubas, P., Wu, F. Q., Lebrun, B., Hisada, M., and Nakajima, T. (1997) *Eur. J. Biochem. 245*, 457−464.
2. Neely, A., and Ling, C. J. (1992) *J. Physiol. (London) 453*, 97−131.
3. Tytgat, J., Chandy, K. G., Garcia, M. L., Gutman, G. A., Martin-Eauclaire, M. F., van der Walt, J. J., and Possani, L. D. (1999) *Trends Pharmacol. Sci. 20*, 444−447.
4. Dai, L., Wu, J. J., Gu, Y. H., Lan, Z. D., Ling, M. H., and Chi, C. W. (2000) *Biochem. J. 346*, 805−809.
5. Selisko, B., Garcia, C., Becerril, B., Gomez-lagunas, F., Garay, C., and Possani, L. D. (1998) *Eur. J. Biochem. 254*, 468−479.
6. Chicchi, G. G., Gimenez-Gallego, G., Ber, E., Garcia, M. L., Winquist, R., and Cascieri, M. A. (1988) *J. Biol. Chem. 263*, 10192−10197.
7. Zerrouk, H., Mansuelle, P., Benslimane, A., Rochatm, H., and Martin-Eauclairem, M. F. (1993) *FEBS Lett. 320*, 189−192.
8. Martins, J. C., Van de Ven, F. J., and Borremans, F. A. (1995) *J. Mol. Biol. 253*, 590−603.
9. Meunier, S., Bernassau, J. M., Sabatier, J. M., Martin-Eauclaire, M. F., Van Rietschoten, J., Cambillau, C., and Darbon, H. (1993) *Biochemistry 32*, 11969−11976.
10. Auguste, P., Hughes, M., Grave, B., Gesquiere, J. C., Maes, P., Tartar, A., Romey, G., Schweitz, H., and Lazdunski, M. (1990) *J. Biol. Chem. 265*, 4753−4759.
11. Sabatier, J. M., Zerrouk, H., Darbon, H., Mabrouk, K., Benslimane, A., Rochat, H., Martin-Eauclaire, M.-F., and Rietschoten, J. Van. (1993) *Biochemistry 32*, 2763−2770.
12. Auguste, P., Hugues, M., Mourre, C., Moinier, D., Tartar, A., and Lazdunski, M. (1992) *Biochemistry 31*, 648−654.
13. Sabatier, J. M., Lecomte, C., Mabrouk, K., Darbon, H., Oughideni, R., Canarelli, S., Rochat, H., Martin-Eauclaire, M.-F.. and Van Rietschoten, J. (1996) *Biochemistry 35*, 10641−10647.
14. Wu, J. J., Dai, L. Lan, Z. D., and Chi, C. W. (1999) *FEBS Lett. 452*, 360−364.
15. Shao, F., Xiong, Y. M., Zhu, R. H., Ling, M. H, Chi, C. W., and Wang, D. C. (1999) *Protein Expression Purif. 17*, 358−365.
16. Schagger, H., and von Jagow, G.(1987) *Anal. Biochem. 166*, 368−379.
17. Zhou, Z., and Misler, S. (1995) *J. Biol. Chem. 270*, 3498−3505.
18. Zhou, Z., and Neher, E. (1993) *J. Physiol. (London) 469*, 245−273.
19. Park, C. S., Hausdorff, S. F., and Miller, C. (1991) *Proc. Natl. Acad. Sci. U.S.A. 88*, 2046−2050.
20. Garcia-Calvo, M., Leonard, R. J., Novick, J., Stevens, S. P., Schmalhofer, W., Kaczorowski, G. J., and Garcia, M. L. (1993) *J. Biol. Chem. 268*, 18866−18874.
21. Legros, C., Feyfant, E., Sampieri, F., Rochat, H., Bougis, P. E., and Martin-Eauclaire, M. F. (1997) *FEBS Lett. 417*, 123−129.
22. Park, Y. B. (1994) *J. Physiol. (London) 481*, 555−570.
23. Martins, J. C., Zhang, W. G., Tartar, A., Lazdunski, M., and Borremans, F. A. (1990) *FEBS Lett. 260*, 249−253.

BI011367Z